Pergamon

Int. J. Heat Mass Transfer. Vol. 38, No. 3, pp. 545–556, 1995

0017-9310/95 $9.50+0.00

0017-9310(94)00173-1

Thermodynamic and optical properties of gases in a wide range of parameters

G. S. ROMANOV, YU. A. STANKEVICH, L. K. STANCHITS and K. L. STEPANOV

Academic Scientific Complex, A. V. Luikov Heat and Mass Transfer Institute of the Academy of Sciences of Belarus, Minsk, Belarus

(*Received* 18 *October* 1993)

Abstract—This work describes calculational methods and the results of systematic calculations of the thermodynamic properties, composition, spectral and mean absorption coefficients for air, water, silicon dioxide and the atmosphere of Mars (0.965 CO_2+0.035 N_2). The range of the considered temperatures from 0.1 to 10^3 eV includes the molecular state of the substances, dissociative gas, low temperature plasma and multicharge plasma. The selected density range $\rho = 10^{-9}$–10^{-2} g cm^{-3} includes the most interesting states for applications. The main mechanisms which determine the absorption coefficients of gases and plasma (inverse bremsstrahlung; photoionization from the ground and excited states of particles; photodissociation of molecules; photoionization from internal particle shells; electronic–vibrational transitions in molecules; line absorption by atoms and ions) were taken into account. Absorption coefficients were determined for photon energies $\varepsilon = 3 \times 10^{-2}$–$10^4$ eV.

1. INTRODUCTION

Knowledge of the thermodynamic and optical properties of a substance is necessary to solve a number of problems in the field of radiative hydrodynamics and plasma dynamics, associated with the investigation of high-temperature hydrodynamic phenomena, such as the entry of space vehicles or meteorites into the atmosphere of planets [1], powerful explosions and high-speed impacts [2, 3], interaction of laser radiation with materials [4, 5], radiative discharge [6], etc. Because of this, it is very important to have data banks containing data on the thermodynamic and optical properties of gases over a wide range of temperatures, densities and photon energies. The use of real characteristics allows one to investigate such phenomena on a quantitative level, which is essential for the creation of new technological processes associated with high energy concentration. At present such data banks exist for air [7–12], some metals and dielectrics [13–18], a number of inert gases [19, 20] and mixtures [21].

The results of systematic calculations of the thermodynamic properties, composition, spectral and average absorption coefficients for air, water, silicon dioxide and the atmosphere of Mars (0.965 CO_2+0.035 N_2) are presented in this paper. The range of temperatures considered, 0.1–10^3 eV, includes the molecular state of the substances, dissociative gas, low temperature plasma and multicharge plasma. The selected range of densities, $\delta = \rho/\rho_0 = 10^{-6}$–$10^1$ (ρ_0 corresponds to the concentration of particles equal to $N_L = 2.687 \times 10^{19}$ cm^{-3}), allows one to make calculations in the most widely used Debye approximation for an equilibrium plasma, and includes the most interesting states for applications. A wide spectral region and detailed spectral descriptions facilitate investigation of the problems of radiation transfer by using the spectral or multigroup approach, and consideration of the interaction of nonthermal radiation with materials.

The results obtained differ substantially from those presented in other publications (e.g. ref. [21]) in that they take into account, firstly, the processes of molecular absorption at low temperatures and, secondly, the contribution of bound–bound transitions of atoms and ions to the absorption value. This allows one to investigate radiation transfer from a hot gas to the surrounding cold space and to consider radiation transport of energy in a high temperature plasma, since line radiation is the principal mechanism of energy losses in high ionized states of a substance [22].

2. THERMODYNAMIC PROPERTIES

Calculations of composition, thermodynamic functions and absorption coefficients were performed on the scale of temperatures enabling one to describe the changes in state of a gas in the processes of dissociation and ionization. To this end, in the temperature range 1000–6000 K, a temperature step of 500 K was selected, in the range $6000 < T < 10\,000$ K the step was 1000 K, and for $10\,000 < T < 20\,000$ K it amounted to 2000 K. The logarithmic scale $\Delta \lg T = 0.1$ was used at higher temperatures (28 isotherms from 1.99 to 10^3 eV). The density step was $\Delta \lg \delta = 0.5$ (15 isochors beginning from $\delta = 10^{-6}$).

Let us briefly discuss the main features of our calculations. The concentrations of particles were determined in accordance with the laws of chemical and ionized equilibrium. For example, in the case of air,

NOMENCLATURE

A	atomic weight
a_0	Bohr radius [cm]
C_4	Stark constant of broadening [$cm^4\ s^{-1}$]
E	internal energy [erg g^{-1}]
E_k	Coulomb energy [erg g^{-1}]
e	charge of electron [$g^{1/2}\ cm^{3/2}\ s^{-1}$]
f_{ij}	oscillator strength
G	free–free Gaunt factor
g	bound–bound Gaunt factor
g_i	statistical weight of i-level
h	Planck's constant [erg s]
I_i	ionization potential [eV]
K_ε	mass coefficient of absorption [$cm^2\ g^{-1}$]
K_P	Planck's mean absorption coefficient [cm^{-1}]
k	Boltzmann constant [erg eV^{-1}]
k_f	extinction coefficient [cm^{-1}]
k_s	scattering coefficient [cm^{-1}]
k_ε	linear coefficient of absorption [cm^{-1}]
L_R	Rosseland mean free path [cm]
m	mass of electron [g]
M	molecular weight, mean molecular weight
n_i	concentration of particle [cm^{-3}]
$q_{v'v''}$	Franck–Condon factor
P	pressure [dn cm^{-2}]
P_k	Coulomb pressure [dn cm^{-2}]
p_{nl}	binding energy of level [eV]
S_{ij}	line strength of transition [g $cm^5\ s^{-2}$]
Ry	Rydberg constant [eV]
T	temperature [eV, K]
z_i	spectroscopic symbol.

Greek symbols

α	fine-structure constant
Γ	nonideality parameter
γ	nonideality parameter
γ_e	Lorentzial width of line [eV]
γ_{ij}	electronic width of line [s^{-1}]
γ_{ef}	adiabatic factor
ΔI_i	lowering of ionization potential [eV]
$\Delta\varepsilon_D$	Doppler width of line [eV]
$\Delta\nu$	width of vibrational band [s^{-1}]
δ	relative density
ε	photon energy [eV]
ν	frequency [s^{-1}]
ρ	density [g cm^{-3}]
Σ_i	partition function
σ_0	cross-section of elastic scattering [cm^2]
σ^{bb}	bound–bound cross-section of absorption [cm^2]
σ^{bf}	bound–free cross-section of absorption [cm^2]
σ^{ff}	free–free cross-section of absorption [cm^2]
χ	nondimensional coefficient defined by equation (9)
ω	cyclic frequency [s^{-1}].

these are N_2, O_2, NO molecules, N_2^+, O_2^+, NO^+ molecular ions, N, O, Ar atoms, their ions and electrons. For the reactions

$$N_2+M \Leftrightarrow N+N+M \quad O_2+M \Leftrightarrow O+O+M$$
$$NO+M \Leftrightarrow N+O+M \quad N+O \Leftrightarrow NO^+ + e$$
$$N+N \Leftrightarrow N_2^+ + e \quad O+O \Leftrightarrow O_2^+ + e \qquad (1)$$

the equations of chemical equilibrium are:

$$(n_N)^2 = F_1 n_{N_2} \quad (n_O)^2 = F_2 n_{O_2}$$
$$n_N n_O = F_3 n_{NO} \quad n_e n_{NO^+} = F_4 n_N n_O$$
$$n_e n_{N_2^+} = F_5 (n_N)^2 \quad n_e n_{O_2^+} = F_6 (n_O)^2. \qquad (2)$$

The concentrations of ions of consecutive ionization stages are described by the Saha equation in the Debye approximation [23]:

$$\frac{n_{i+1} n_e}{n_i} = 2\frac{\sum_{i+1}}{\sum_i}\left(\frac{4\pi m k T}{h^2}\right)^{3/2} \exp\left(-\frac{I_i - \Delta I_i}{kT}\right). \qquad (3)$$

The equilibrium constants in equations (2)–(3) are determined by a set of atomic and molecular characteristics. Their values, particularly energy levels, statistical weights, dissociation and ionization energies etc. were defined according to refs. [24–27].

The lowering of ionization energy due to the Coulomb interaction of particles is

$$\frac{\Delta I_i}{kT} = \ln\frac{(1+\gamma/2)[1+(z_i+1)^2\gamma/2]}{(1+z_i^2\gamma/2)} \qquad (4)$$

where z_i is the ion charge of species i ($i = 1$ is for a neutral atom), γ is determined as a positive root of the equation

$$\gamma^2 = \left(\frac{e^2}{kT}\right)^3 4\pi \sum \frac{n_i z_i^2}{1+z_i^2\gamma/2}. \qquad (5)$$

For a slightly nonideal plasma, the magnitude of γ coincides with the ordinary nonideality parameter,

$$\Gamma = \frac{e^2}{kTr_D} = \left(\frac{e^2}{kT}\right)^{3/2} \left\{4\pi\left(\sum n_i z_i^2 + n_e\right)\right\}^{1/2}. \qquad (6)$$

The statistical sums of atoms and ions are calculated in accordance with the Planck–Larkin approach

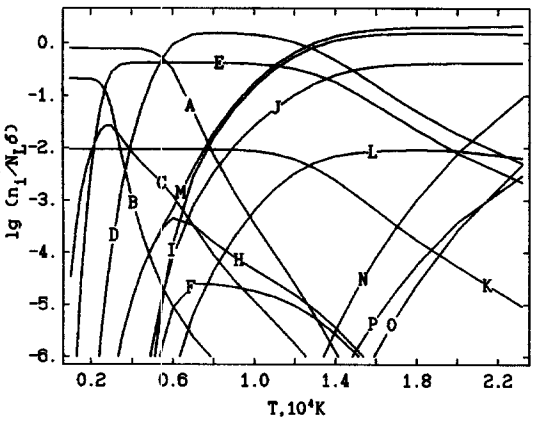

Fig. 1. Composition of air plasma vs T at $\delta = 10^{-3}$. (A) N_2, (B) O_2, (C) NO, (D) N, (E) O, (F) N_2^+, (H) NO^+, (I) N^+, (J) O^+, (K) Ar, (L) Ar^+, (M) e, (N) N^{2+}, (O) O^{2+}, (P) Ar^{2+}.

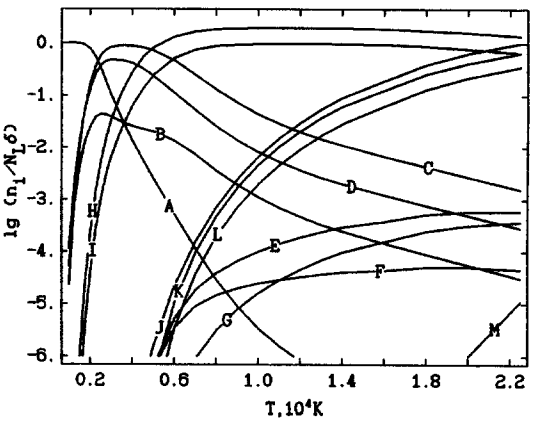

Fig. 2. Composition of steam vs T at $\delta = 1$. (A) H_2O, (B) O_2, (C) OH, (D) H_2, (E) OH^+, (F) O_2^+, (G) H_2^+, (H) H, (I) O, (J) e, (K) H^+, (L) O^+, (M) O^{2+}.

$$\sum_i = \sum g_{ij} \exp(-E_{ij}/kT) W_{ij} \tag{7}$$

$$W_{ij} = 1 - \left(1 + \frac{I_i - E_{ij}}{kT}\right) \exp\left(\frac{E_{ij} - I_i}{kT}\right).$$

The thermodynamic characteristics (density, pressure, specific internal energy, effective adiabatic factor) are determined by the formulae

$$\rho = 1.67 \times 10^{-24} \sum n_i A_i, \quad P = kT \sum n_i - P_k$$

$$E = \frac{3kT}{2\rho} \sum n_i + \frac{kT}{2\rho} \sum_m n_m q_m$$

$$+ \frac{1}{\rho} \sum_m n_m \sum_v \frac{h\omega g_v}{\exp(h\omega/kT) - 1} + \frac{1}{\rho} \sum n_i (Q_i + \bar{\varepsilon}_i) - E_k$$

$$\gamma_{ef} = 1 + \frac{P}{\rho E} \tag{8}$$

where A_i is the atomic weight, Q_i and $\bar{\varepsilon}_i$ are the energy of formation of particles and the mean energy of their excitation, respectively, q_m and g_v are the number of the rotational degrees of freedom of a molecule and the statistical weight of its vibrational mode, respectively. The Coulomb corrections to the thermodynamic functions have the form

$$P_k = \frac{kT\chi^3}{24\pi} \quad E_k = \frac{kT\chi^3}{8\pi\rho} \quad \chi = \gamma \frac{kT}{e^2}. \tag{9}$$

In view of a large vaporization heat of silicon dioxide, the thermodynamic equilibrium of vapor with the condensed phase was considered. Therefore, at temperatures below 6000 K, the vapor density was restricted from above by its value on the vapor-condensed phase boundary [28].

Some of the results obtained are illustrated in Figs. 1 and 2, showing the composition of gases as a function of temperature. All the components are presented in non-dimensional form, $\bar{n} = n/\delta N_L$. Thus, when $T \to 0$, the sum of all the particles is equal to 1. With an increase in temperature, the full particle concentration also increases due to dissociation and ionization.

It is interesting to note that, at low temperatures, the electron concentration is determined by concentrations of molecular ions (NO^+ for air and for the atmosphere of Mars, O_2^+ for steam and SiO^+ in silicon dioxide). It is seen that the interval of temperatures in which molecules are present is considerably expanded with the growth in density, and the gas properties appear to be dependent on an ever-growing number of components.

Note that the equations of chemical equilibrium were solved with the help of the relaxation method. In the absence of molecules, the system of Saha equations was solved by using the iterative method where the temperature and the electron density were selected as independent variables [29].

Table 1 shows the influence of the density of gas on its properties. It lists the values of pressure P, internal energy E, adiabatic factor γ_{ef}, mean molecular weight M and concentration of particles $\bar{n}_i = n_i/\delta N_L$ for several isotherms of the atmosphere of Mars.

The dependence of the thermodynamic values of silicon dioxide on temperature for a number of densities is presented in Fig. 3. The curves A, B, ... H correspond to the change in density from $\delta = 10^{-6}$ to 10^1 every other order of magnitude. The figure also illustrates the saturation curve for the vapor and condensed phases of SiO_2 [28]. The dependence of the saturation density and pressure on temperature for SiO_2 is given in Table 2.

For gas-dynamic applications, it is often necessary to represent the data as functions of the variables ρ and E. Interpolation of the results to the planes of new independent variables leads to the loss of accuracy, especially in the range of parameters corresponding to the pauses of dissociation and ionization. Therefore, the gas characteristics were tabulated as depending on ρ–T, as well as ρ–E. Figure 4 shows the behaviour of these values as functions of E–ρ for air.

Table 1. Composition of the atmosphere of Mars as a function of density

δ	1.00−06	1.00−04	1.00−02	1.00+00
		$T = 3000$ K		
P	2.18+01	2.09+03	1.57+05	1.25+07
E	1.43+11	1.34+11	7.92+10	4.51+10
γ_{ef}	1.08+00	1.08+00	1.10+00	1.14+00
M	2.21+01	2.31+01	3.08+01	3.88+01
e	9.76−07	2.81−07	3.91−08	3.08−09
CO_2	2.69−04	2.25−02	3.15−01	7.37−01
CO	9.65−01	9.43−01	6.50−01	2.28−01
N_2	3.43−02	3.24−02	2.99−02	3.15−02
O_2	7.82−04	5.72−02	2.36−01	1.05−01
NO	6.27−04	5.21−03	1.02−02	6.96−03
N	7.80−04	7.58−05	7.29−06	7.48−07
O	9.63−01	8.23−01	1.67−01	1.12−02
C	2.27−07	2.60−09	8.81−11	4.64−12
		$T = 30\,000$ K		
P	1.07+03	9.33+04	6.99+06	5.44+08
E	4.93+12	3.75+12	2.12+12	1.43+12
γ_{ef}	1.11+00	1.13+00	1.17+00	1.20+00
M	4.53+00	5.16+00	6.82+00	8.40+00
e	6.62+00	5.45+00	3.40+00	2.20+00
CO	4.11−28	3.59−18	1.04−10	2.06−05
N_2	8.15−31	4.99−21	1.58−13	2.60−08
O_2	1.00−26	2.79−17	1.51−10	1.71−05
C_2	2.10−30	5.74−20	9.00−12	3.10−06
N	9.79−11	7.66−07	4.30−04	1.75−02
O	1.44−08	7.62−05	1.77−02	5.96−01
C	1.32−10	2.18−06	2.73−03	1.61−01
N^{1+}	6.45−05	6.19−03	5.88−02	5.23−02
O^{1+}	7.11−03	4.60−01	1.81+00	1.33+00
C^{1+}	1.44−04	2.91−02	6.17−01	7.93−01
N^{2+}	5.36−02	6.36−02	1.07−02	2.49−04
O^{2+}	1.84+00	1.47+00	1.03−01	1.98−03
C^{2+}	3.66−01	9.17−01	3.45−01	1.16−02
N^{3+}	1.63−02	2.42−04	7.51−07	4.47−10
O^{3+}	8.64−02	8.62−04	1.11−06	5.47−10
C^{3+}	5.98−01	1.87−02	1.29−04	1.11−07
C^{4+}	5.78−04	2.27−07	2.94−11	6.02−16

3. OPTICAL PROPERTIES

Let us now turn to discussion of the optical properties of gases. The spectral absorption coefficients were determined for the photon energies $\varepsilon = 3 \times 10^{-2}$–$10^4$ eV. The following spectral intervals were chosen: the $\varepsilon \leqslant 17.354$ eV range contained 560 intervals with a step of 250 cm^{-1} [9]; beginning from $\varepsilon = 17.354$ eV, the logarithmic scale of energy was used, for which the energy step is determined as $\Delta\varepsilon = \varepsilon_0 10^{(i-560)/500}$, where $\varepsilon_0 = 8.010259 \times 10^{-2}$ eV. Thus the full spectral scale included 1941 intervals.

In order to determine the absorption coefficients, it is necessary to summarize the contributions of different types of transitions (free–free, bound–free, bound–bound) from many particles. The dominant processes vary considerably with temperature and depend on the spectral interval. The main mechanisms which determine the absorption coefficients of gases and plasma are: inverse bremsstrahlung; photoionization from the ground and excited states of particles; photodissociation of molecules; photoionization from the internal shells of particles; electronic–vibrational transitions in molecules; and line absorption by atoms and ions. The contribution of just-cited processes was determined using the following approximations.

The cross section for free–free transitions in the fields of a neutral particle was expressed in terms of the electron elastic scattering cross-section σ_0. For atoms the formula obtained in ref. [30] was used

$$\sigma^{ff}(\varepsilon) = \frac{16\sqrt{2}}{3\sqrt{\pi}} \alpha\pi a_0^3 \sigma_0 \left(\frac{Ry}{\varepsilon}\right)^{3/2} \times \left(\frac{\varepsilon}{2kT}\right)^{1/2} \exp\left(\frac{\varepsilon}{2kT}\right) K_2\left(\frac{\varepsilon}{2kT}\right). \quad (10)$$

Here $\alpha = 2\pi e^2/hc$, $K_2(x)$ is the Bessel function of an imaginary argument. Inverse bremsstrahlung on molecules was determined by analogy with refs. [31, 32]:

$$\sigma^{ff}(\varepsilon) = 32\frac{\sqrt{2}}{\sqrt{\pi}} \alpha a_0 \pi a_0^2 \sigma_0 \left(\frac{Ry}{\varepsilon}\right)^3 \left(\frac{kT}{Ry}\right)^{3/2} \left(1 + \frac{3\varepsilon}{4kT}\right). \quad (11)$$

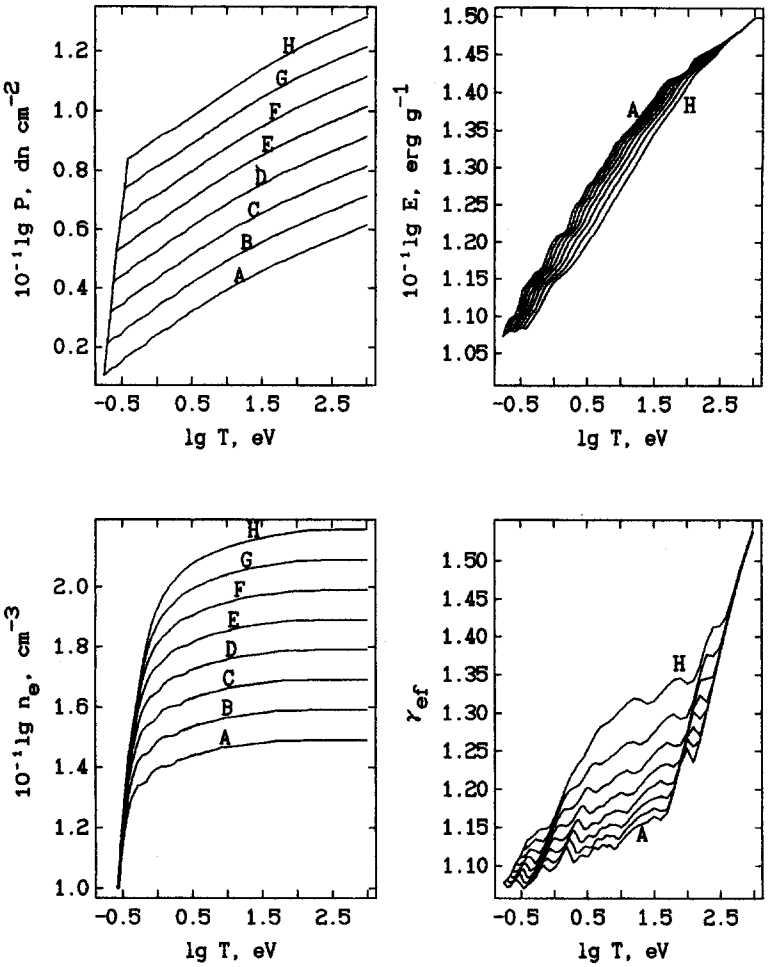

Fig. 3. Thermodynamic properties of silicon dioxide.

Absorption in the process of electron scattering on an ion was calculated according to the Kramers approximation with the use of the Gaunt factor [33],

$$\sigma^{\mathrm{ff}}(\varepsilon) = \frac{256\sqrt{\pi}}{3\sqrt{3}} \alpha a_0 (\pi a_0^2) i^2 \left(\frac{Ry}{kT}\right)^{1/2} \left(\frac{Ry}{\varepsilon}\right)^3 G(T, \varepsilon). \tag{12}$$

Different approaches were employed for describing bound–free processes. For N and O atoms and their ions in the ground state and low levels of the basic configuration, the corresponding cross-sections were found with the help of the Hartree–Fock method [34]. Table 3 presents a list of states for which the photoionization cross-sections were tabulated.

The cross-sections of hydrogen and H-like ions are calculated by exact formulae [35] for $n \leqslant 4$. For C, Si and their ions, the cross-sections for all the levels were calculated using the quantum defect method [36]:

$$\sigma_{nl}^{\mathrm{bf}}(\varepsilon) = \frac{4\alpha}{3} \pi a_0^2 \left(\frac{\varepsilon}{Ry}\right) \left(\frac{Ry}{p_{nl}}\right)^2 \sum_{l' = l \pm 1} C_{l'} |g_{ll'}|^2 \tag{13}$$

where $p_{nl} = Z^2 Ry / n_l^{*2}$ is the electron-binding energy of level nl, $C_{l'}$ is the factor dependent on the spin and orbital momentum of the system in the initial and final

Table 2. The temperature dependence of density and pressure saturation for SiO_2

T [K]	2000	2500	3000	3500	4000	4500	5000
ρ [g cm^{-3}]	2.55−9	1.16−6	3.86−5	5.75−4	4.16−3	1.84−2	5.74−2
P [atm]	1.32−5	6.80−3	2.64−1	4.40+0	3.62+1	1.78+2	6.15+2

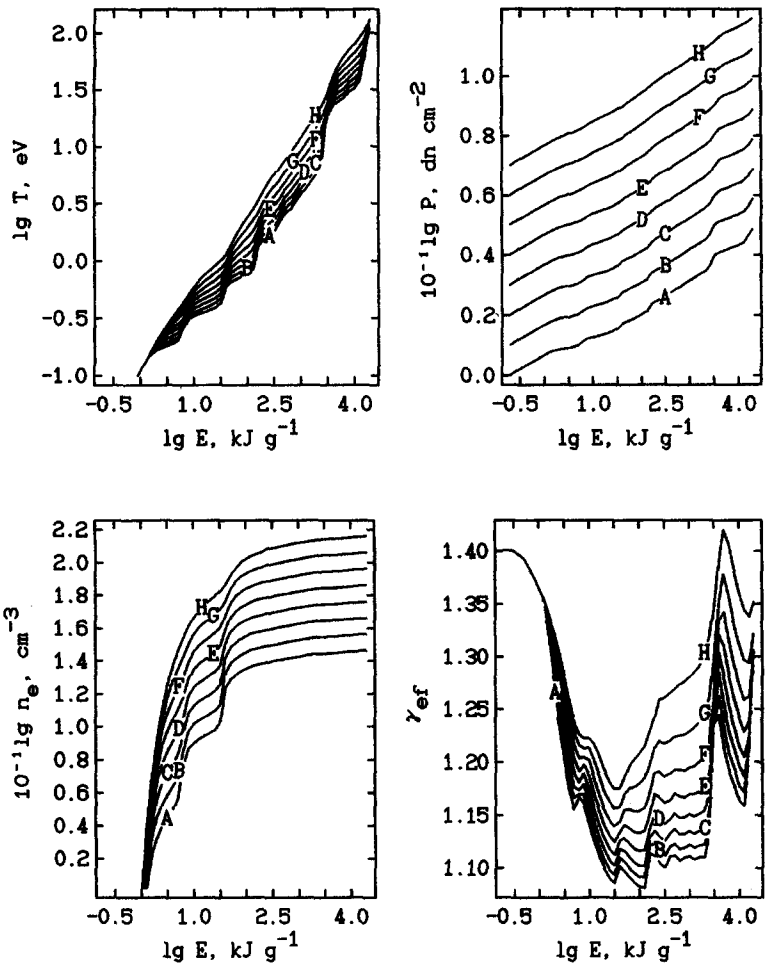

Fig. 4. Thermodynamic properties of air as functions of E for various ρ.

Table 3. Configurations of atoms and ions with tabulated photoionization cross-sections

Ion	State	Residual ion state	Ion	State	Residual ion state
N I			O I		
1	$2s^22p^3\ ^4S$	$2s^22p^2\ ^3P$	1	$2s^22p^4\ ^3P$	$2s^22p^3\ ^4S, ^2P, ^2D$
2	$2s^22p^3\ ^2D$	$2s^22p^2\ ^3P, ^1D$	2	$2s^22p^4\ ^1D$	$2s^22p^3\ ^2P, ^2D$
3	$2s^22p^3\ ^2P$	$2s^22p^2\ ^3P, ^1D, ^1S$	3	$2s^22p^4\ ^1S$	$2s^22p^3\ ^2P$
N II			O II		
1	$2s^22p^2\ ^3P$	$2s^22p\ ^2P$	1	$2s^22p^3\ ^4S$	$2s^22p^2\ ^3P$
2	$2s^22p^2\ ^1D$	$2s^22p\ ^2P$	2	$2s^22p^3\ ^2D$	$2s^22p^2\ ^3P, ^1D$
3	$2s^22p^2\ ^1S$	$2s^22p\ ^2P$	3	$2s^22p^3\ ^2P$	$2s^22p^2\ ^1S, ^3P, ^1D$
N III			O III		
1	$2s^22p\ ^2P$	$2s^2\ ^1S$	1	$2s^22p^2\ ^3P$	$2s^22p\ ^2P$
2	$2s2p^2\ ^4P$	$2s2p\ ^3P$	2	$2s^22p^2\ ^1D$	$2s^22p\ ^2P$
3	$2s2p^2\ ^2D$	$2s2p\ ^3P, ^1P$	3	$2s^22p^2\ ^1S$	$2s^22p\ ^2P$
N IV			O IV		
1	$2s^2\ ^1S$	$2s\ ^2S$	1	$2s^22p\ ^2P$	$2s^2\ ^1S$
2	$2s2p\ ^3P$	$2s\ ^2S$	2	$2s2p^2\ ^4P$	$2s2p\ ^3P$
3	$2s2p\ ^1P$	$2s\ ^2S$	3	$2s2p^2\ ^2D$	$2s2p\ ^3P$
N V			O V		
1	$2s\ ^2S$	$1s^2\ ^1S$	1	$2s^2\ ^1S$	$2s\ ^2S$
2	$2p\ ^2P$	$1s^2\ ^1S$	2	$2s2p\ ^3P$	$2s\ ^2S$
N VI			3	$2s2p\ ^1P$	$2s\ ^2S$
1	$1s^2\ ^1S$	$1s\ ^2S$	O VI		
O VII			1	$2s\ ^2S$	$1s^2\ ^1S$
1	$1s^2\ ^1S$	$1s\ ^2S$	2	$2p\ ^2P$	$1s^2\ ^1S$

states; the function g is related to the radial integral as

$$g_{ll'} = \left(\frac{p_{nl}}{Ry}\right)\int_0^\infty R_{nl}(r)R_{El'}(r)r\,dr = \frac{G_{ll'}(n_l^*)}{\sqrt{\gamma_s(n_l^*)}}\left(\frac{\varepsilon}{p_{nl}}\right)^{-\gamma_{ll'}}\cos\pi(n_l^*+\mu_{l'}(E)+\chi_{ll'}).$$

Here E is the kinetic energy of a photoelectron, n_l^* is the effective quantum number of the nl-level; $\mu_l = n - n_l^*$ is the nl series quantum defect; $\mu_l(E)$ is the quantum defect of the $n'l'$ series, which is extrapolated in the region of positive energies; functions $G_{ll'}$, $\gamma_{ll'}$, $\chi_{ll'}$, ζ are tabulated in ref. [36]. The photoionization cross-section of all the particles from excited states with the principal quantum number n, which is greater than that of the ground state of the outer electron, was calculated by applying the quantum defect method. The H-like approximation

$$\sigma_{nl}^{bf}(\varepsilon) = \frac{64}{3\sqrt{3}}\alpha\pi a_0^2\frac{p_{nl}Ry}{n\varepsilon^3} \tag{14}$$

was used for levels which have a small binding energy and for levels with orbital number $l \geqslant 3$. The Hartree–Fock–Sleter method [37] was used to calculate the innershell photoionization cross-sections.

The stepped approximation based on the experimental data of refs. [38, 39] was used to calculate the photoionization of the H_2, CO, C_2, CN molecules:

$$\sigma^{bf}(\varepsilon) = \begin{cases} 0, & \varepsilon < \varepsilon_p \\ \sigma_p, & \varepsilon \geqslant \varepsilon_p \end{cases}. \tag{15}$$

The parameters ε_p and σ_p are given in Table 4.

The photoionization cross-sections of N_2, O_2, NO were calculated in accordance with ref. [40]; they were determined under atmospheric conditions. Their averaging gives the following expressions (ε in eV, $\sigma \times 10^{18}$) [39]:

Table 4. The photoionization cross-section parameters

	H_2	CO	C_2	CN
ε_p, [eV]	15.43	14.22	12.00	14.61
$\sigma_p(10^{-18})$ [cm^2]	7.00	15.00	10.00	5.00

In the harder region of the spectrum, the molecular absorption cross-sections were calculated in terms of the atomic cross-sections on the assumption of their additivity [41].

In accordance with ref. [42], the molecular photoionization absorption cross-section can be represented as

$$\sigma^{bf}(\varepsilon) = \frac{1}{3}\pi a_0^2\alpha^2\left(\frac{\varepsilon}{Ry}\right)R_e^2(\varepsilon) \times \sum_{v',v''} W_{v''}(T)q_{v''}(\varepsilon)\varphi(\varepsilon-\varepsilon_{v',v''}) \tag{17}$$

where $W_{v''}$ is the Boltzmann probability of particle existence on the v'' level, $q_{v''}(\varepsilon)$ is the Franck–Condon factor for transitions between the vibrational levels of the neutral molecule and residual ion, R_e^2(a.u.) is the electron part of the transition dipole moment, and φ takes into account the v''–v' transition threshold and its frequency-dependence. In the present calculations, simple approximations were used, e.g. for the O_2 molecule [40],

$$\sigma_{O_2} = \begin{cases} 0.4 & 9.456 < \varepsilon \leqslant 9.745 \\ 2.2 & 9.238 < \varepsilon \leqslant 9.456 \\ 7.0 & 9.036 < \varepsilon \leqslant 9.238 \\ 12.0 & 8.160 < \varepsilon \leqslant 9.036 \\ 12\exp[-189.66(\varepsilon^{-1} - 0.1225)] & 7.083 < \varepsilon \leqslant 8.160 \end{cases} \tag{18}$$

$$\sigma_{N_2} = \begin{cases} 2.5+338.416(\varepsilon^{-1}-1) & 16.487 < \varepsilon \leqslant 61.980 \\ 17.5\exp[-298.75(\varepsilon^{-1}-0.0605)] & 14.750 < \varepsilon \leqslant 16.487 \\ 1 & 12.396 < \varepsilon \leqslant 14.750 \end{cases}$$

$$\sigma_{O_2} = \begin{cases} 30 & 15.495 < \varepsilon \leqslant 26.400 \\ 7 & 14.578 < \varepsilon \leqslant 15.495 \\ 10\exp[-142.56(\varepsilon^{-1}-0.06857)] & 11.806 < \varepsilon \leqslant 14.578 \\ 0.3 & 9.669 < \varepsilon \leqslant 11.806 \end{cases}$$

$$\sigma_{NO} = \begin{cases} 7.5+387.80(\varepsilon^{-1}-0.016134) & 20.676 < \varepsilon \leqslant 61.980 \\ 20-1053.75(\varepsilon^{-1}-0.048402) & 15.495 < \varepsilon \leqslant 20.676 \\ 3.0+1756.5(\varepsilon^{-1}-0.06454) & 13.475 < \varepsilon \leqslant 15.495 \\ 20\exp[-97.72(\varepsilon^{-1}-0.07422)] & 10.326 < \varepsilon \leqslant 13.475 \\ 2.2 & 8.729 < \varepsilon \leqslant 10.326. \end{cases} \tag{16}$$

Table 5. The quantity of levels and lines for the components of air

	Ion	1	2	3	4	5	6	7	8
N	levels	18	21	32	20	12	18	10	
	lines	37	78	54	51	83	125	45	
O	levels	16	35	40	27	30	12	18	10
	lines	37	59	61	61	55	83	125	45
	Ion					15	16	17	18
Ar	levels					30	25	22	10
	lines					66	42	46	45

When calculating absorption in the atom and ion spectral lines, the profile of the latter was specified as having the Voigt shape (the electron impact broadening and thermal Doppler effect were accounted for in this case),

$$\sigma_{ij}^{bb}(\varepsilon) = \frac{\pi e^2 h}{mc} f_{ij}\varphi(\varepsilon) \tag{19}$$

$$\varphi(\varepsilon) = \frac{1}{\sqrt{(\pi)}\,\Delta\varepsilon_D} H(a,u)$$

$$H(a,u) = \frac{a}{\pi}\int_{-\infty}^{+\infty} \frac{\exp(-y^2)\,dy}{a^2+(u-y)^2}. \tag{20}$$

Here f_{ij} is the transition oscillator strength; $a = \gamma_e/2\Delta\varepsilon_D$ is the collisional half-width to Doppler width ratio; $\Delta\varepsilon_D = \varepsilon_0(2kT/Mc^2)^{1/2}$; $u = (\varepsilon-\varepsilon_0)/\Delta\varepsilon_D$. The electron half-width of lines was calculated according to ref. [43]: for neutrals

$$\frac{\gamma_{ij}}{2} = 11.4\left(\frac{8kT}{\pi m}\right)^{1/6} n_e C_4^{2/3} \tag{21}$$

$$C_4^{ij} = \frac{2\pi e^2}{3h^2}\sum_l \left[\frac{S_{il}}{g_i\omega_{il}} + \frac{S_{jl}}{g_j\omega_{jl}}\right]$$

for ions

$$\frac{\gamma_{ij}}{2} = 8\left(\frac{\pi}{3}\right)^{3/2}\frac{ha_0}{2\pi m}\left(\frac{Ry}{kT}\right)^{1/2}$$

$$\times n_e\left[\sum_l |\langle i|\bar{r}|l\rangle|^2 g\left(\frac{3kT}{2|E_i-E_l|}\right)\right.$$

$$\left.+\sum_l |\langle j|\bar{r}|l\rangle|^2 g\left(\frac{3kT}{2|E_j-E_l|}\right)\right]. \tag{22}$$

All the dipole transitions from the initial i and final j states make contributions to the broadening.

Table 5 presents information on the quantity of individually incorporated levels and lines for different components of the air plasma.

It should be noted that in calculations the air was assigned as a mixture of gases with the volume ratio of components N_2 0.7812, O_2 0.2095, Ar 0.0093. Only multicharge ions of argon were used, since the contribution of argon to absorption is appreciable at high temperatures only when N and O are fully ionized. This table specifies the numbers of transitions in continuous and discrete spectra, which were included in these calculations.

The absorption cross-section of the electronic–vibrational transition of diatomic molecules was calculated using an approximate method, which employs the expression for integral absorption in the band of electronic–vibrational transitions (per particle) [44]:

$$\kappa^{bb}(\nu) = \frac{4\pi}{3}\pi a_0^2\alpha\frac{kTq_{v'v''}}{Q(T)B_{v''}}\nu S_e$$

$$\times\exp\left(-\frac{E_{e'}+E_{v''}}{kT}\right)\left[1-\exp\left(-\frac{h\nu}{kT}\right)\right]. \tag{23}$$

Here $B_{v''}$ is the rotational constant of the lower level, $q_{v'v''}$ is the Franck–Condon factor, $Q(T)$ is the statistical sum over the inner degrees of freedom of a molecule, S_e(a.u.) is the strength of electron transition, ν is the frequency. Division of equation (23) by the width of the vibrational band, $\Delta\nu = (\nu_{e'}+\nu_{e''})/2$, yields the average cross-section of absorption in the band $v'v''$. Table 6 gives the electronic–vibrational bands, which were taken into account in calculations. The data necessary for calculation are taken from refs. [26, 32, 39, 45].

To calculate the contribution to absorption of three-atom CO_2 and H_2O molecules, the experimental information on cold absorption coefficients [46, 47] and data on temperature-dependences of cross-sections at separate spectral intervals [48, 49] were used.

Detailed information about the spectral and mean absorption coefficients is presented in ref. [50]. Let us consider some results of the present calculations.

The temperature dependence of the air absorption coefficient in the region of states, when k_ε is determined by atoms and ions and when the role of molecules is negligibly small, is illustrated in Fig. 5. It is seen that, with a raise in temperature, the absorption caused by the optical shell electron transitions increases for low energy quanta and decreases for high energy quanta. Such behavior of this coefficient is typical for a multicharge plasma where bremsstrahlung processes determine the absorption of photons with $\varepsilon \approx T$, and photoionization processes determine the absorption of harder photons.

Table 6. Electronic-vibrational bands of diatomic molecules

O	Schumann–Runge	C_2	Swan
			Millikan
N_2	first positive		Deslandres
	second positive		Fox–Herzberg
	Birge–Hopfield 1		Freymark
	Birge–Hopfield 2		
	Lyman–Birge–Hopfield	CO	4th positive
			Angstrom
NO	β	CO^+	comet tails
	γ		first negative
	δ		
	ε	CN	fundamental red
	ε'		violet
N_2^+	Meinel	OH	violet
	first negative		
		H_2	two Lymen
			two Verner
SiO	violet		

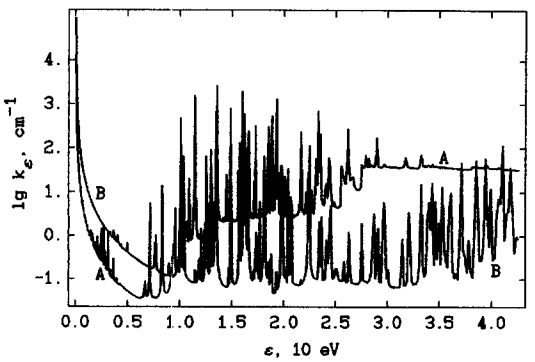

Fig. 5. Absorption coefficient of air at $\delta = 10^{-1}$. (A) $T = 3 \times 10^4$ K; (B) 10^5.

The mass absorption coefficient $K_\varepsilon = k_\varepsilon/\rho$ is frequently used instead of the linear coefficient for solving the problems of radiation gas dynamics. The mass coefficient has a weak density dependence, which is convenient for the interpolation of spectral characteristics by ρ. The following results are obtained for the mass coefficient K_ε.

Figure 6 illustrates calculations of the absorption coefficients of the atmosphere of Mars. The contributions of molecular components (curve B), atoms and ions (C) to the full absorption coefficient (A) are shown at $T = 8 \times 10^3$ K and $\delta = 10^{-2}$. In fact, the total absorption for $\varepsilon > 2$ eV at the points located beyond the spectral lines is basically determined by molecular absorption.

An example of calculation of the absorption spectrum for water is presented in Fig. 7. The results were obtained on the above-described energy scale containing 1941 spectral intervals.

Figures 8 and 9 illustrate the results of calculations of the Planck mean opacities and Rosseland mean free paths. It is appropriate to use the Planck mean absorption coefficient to calculate the emission from an optically thin gas. Under the conditions where a gas volume is fairly opaque, the Rosseland mean free path is frequently used in radiation transport considerations. Curves 1–15 fit the relative densities $\delta = 10^{-6}$–10^{1} with half-order steps. In these calculations the radiation scattering on free electrons was accounted for, thus limiting the magnitudes of mean values at high temperatures (full ionization) and low densities:

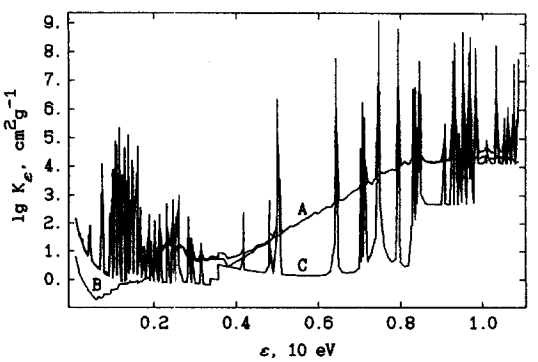

Fig. 6. Absorption coefficient of the Mars atmosphere. $T = 8 \times 10^3$ K, $\delta = 10^{-2}$.

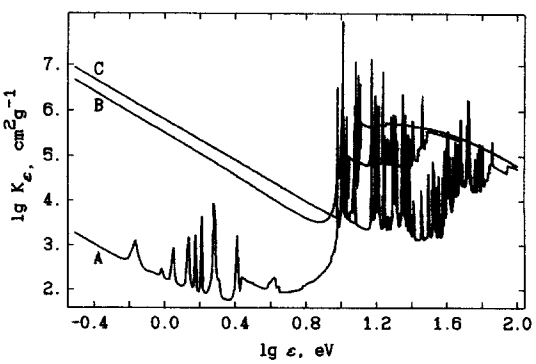

Fig. 7. Absorption coefficient of water. $\delta = 10^0$, (A) $T = 1$ eV, (B) 3.16 eV, (C) 10 eV.

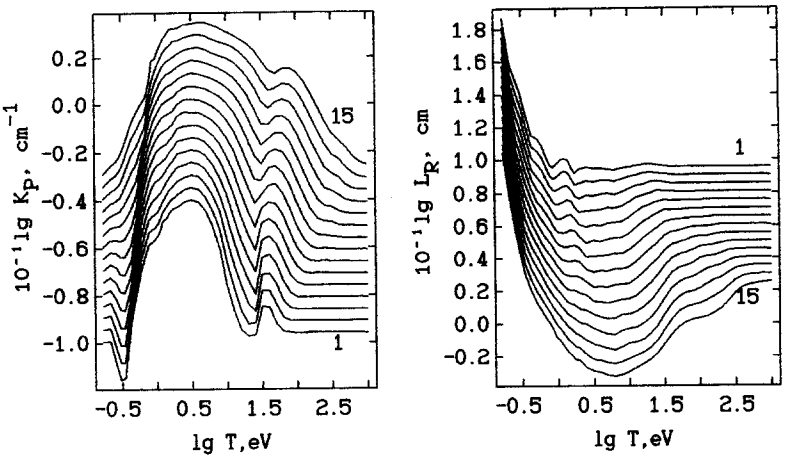

Fig. 8. Planck and Rosseland mean opacities in air.

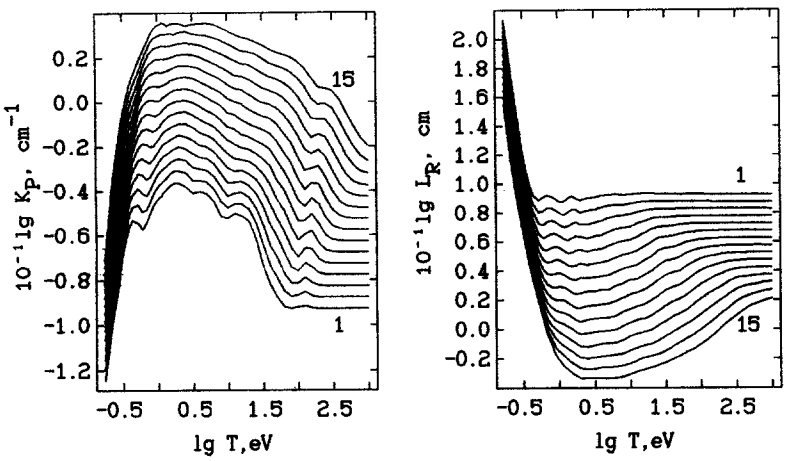

Fig. 9. Planck and Rosseland mean opacities in silicon dioxide.

$$K_P = \frac{15}{\pi^4}\int_0^\infty k_f(x)\frac{x^3 e^{-x}}{1-e^{-x}}dx$$

$$L_R = \frac{15}{4\pi^4}\int_0^\infty \frac{dx}{k_f(x)}\frac{x^4 e^{-x}}{(1-e^{-x})^2} \qquad (24)$$

where $k_f = k(x) + k_s$, $k(x) = k(\varepsilon/T)$ is the absorption coefficient, and the scattering coefficient k_s is defined by

$$k_s = \frac{8\pi}{3}a_0^2\alpha^4 n_e. \qquad (25)$$

Let us briefly discuss the limits of the applicability of the data obtained. At high densities these data are restricted by the manifestation of nonideality effects (at temperatures $T \approx 1$ eV and densities $\delta \approx 1$) when $\gamma \approx 1$. In this case, the calculation of the thermodynamic properties and composition with the use of the Debye approximation may be considered as a reasonable extrapolation to the region of strong nonideality. In the remaining region of $T-\delta$, this approximation is quite applicable.

The nonideality influences the optical properties of plasma causing broadening, merging and transition to a continuous spectrum of some excited levels of a discrete spectrum [50]. Besides, due to the action of the plasma microfield, the probability for the realization of certain states decreases [23]. The first effect shifts the photoionization threshold to smaller energies and increases the absorption coefficient $\exp(h\Delta\nu/kT)$ times on average. The second effect causes decrease of absorption in the long-wave region, due to the decrease in the photoionization contribution of unrealized levels. Although these effects cause deviation from the ideal spectrum in different intervals of quantum energy, the second effect neutralizes the first one, since the broadened lines and those shifted to continuum turn out to be unrealized in the vicinity of the photoionization threshold. In turn, the bremsstrahlung processes make a large contribution to the absorption of quanta with the energy $\varepsilon < T$ and therefore the role of the level nonrealization is not predominant. Besides, this spectral region is not the most important one in thermal radiation transfer. Calculation of optical properties without account for nonideality is justified, due to the reasons stated above

and to the absence of a workable theory for the effect of nonideality on the optical characteristics of plasma.

4. CONCLUSION

In the present study the following results were obtained:

(1) the composition and thermodynamic functions of air, water, silicon dioxide and the atmosphere of Mars at temperatures from 0.1 to 10^3 eV and densities 10^{-9}–10^{-2} g cm^{-3};

(2) the spectral coefficients of continuous absorption; these were determined on the floating scale of energy, including the absorption thresholds of particles; these data make it possible to average spectra over any spectral intervals;

(3) integral absorption in each line at given T and δ; the constants of line broadening which are necessary to account for the contribution of the lines to total absorption at averaging over spectral intervals;

(4) the total spectral absorption coefficients which allow one to resolve separate features of a spectrum, such as line profiles;

(5) the total small-group absorption coefficients for quanta with energies from 3×10^{-2} to 10^4 eV (1941 spectral groups);

(6) the group mean absorption coefficients; the data mentioned in the previous item allow one to calculate the group mean absorption coefficients for arbitrary division of a spectrum into groups;

(7) the Planck mean and Rosseland mean group and integral absorption coefficients and paths;

(8) the data on the absorption cross-section of separate components in the region of their existence, which allow the estimation of their contribution to total absorption depending on temperature, density and energy.

Acknowledgement—This work was supported, in part, by a Soros Foundation Grant awarded by the American Physical Society.

REFERENCES

1. V. A. Bronshten, *Physics of Meteorite Phenomena.* Nauka, Moscow (1976).
2. *Action of Nuclear Explosion* (Edited by S. S. Grigorjan and G. S. Shapiro). Mir, Moscow (1971).
3. *Highvelocity Shock Phenomena* (Edited by V. N. Nikolaevskii). Mir, Moscow (1973).
4. S. I. Anisimov, Ya. A. Imas, G. S. Romanov and Yu. V. Khodyko, *Action of High Power Radiation on Metals.* Nauka, Moscow (1970).
5. Yu. P. Raizer, *Laser Spark and Extension of Discharges.* Nauka, Moscow (1974).
6. V. A. Burtsev, N. V. Kalinin and A. V. Luchinskii, *Electrical Explosion of Conductors and Its Application in Electrophysical Devices.* Energoatomizdat, Moscow (1990).
7. N. M. Kuznetsov, *Thermodynamic Functions and Shock Adiabatics of Air.* Mashinostroyeniye, Moscow (1965).
8. R. K. M. Landshoff and J. L. Magee, *Thermal Radiation Phenomena,* Vols 1, 2. IFI/Plenum, New York (1969).
9. I. V. Avilova, L. M. Biberman, V. S. Vorobiov and V. M. Zamalin, *Optical Properties of Hot Air.* Nauka, Moscow (1970).
10. G. A. Kobsev, Optical properties of air plasma under high temperatures, Preprint No. 1-112 of the Institute for High Temperatures, Moscow (1983).
11. G. A. Kobsev and V. A. Nuzhny, Spectral and integral optical characteristics of continuous spectrum of air plasma under high temperatures, Preprint No. 1-131 of the Institute for High Temperatures, Moscow (1984).
12. G. A. Kobsev and V. A. Nuzhny, Optical properties of air plasma with account for spectral lines, $T = 20\,000$–$30\,000$ K, Preprint No. 1-134 of the Institute for High Temperatures, Moscow (1984).
13. N. N. Kalitkin, L. V. Kuz'mina and V. S. Rogov, *Tables of Thermodynamic Functions and Transport Coefficients of Plasma.* Institute of Applied Mathematics, Academy of Science of the U.S.S.R. (1972).
14. B. V. Zamyshlyaev, E. L. Stupitsky and A. G. Guz', *Composition and Thermodynamic Functions of Plasma.* Energoatomizdat, Moscow (1984).
15. V. K. Gryaznov, I. L. Iosilevskii and Yu. G. Krasnikov, *Thermophysical Properties of the Gas-phase Nuclear Reactor Media.* Atomizdat, Moscow (1980).
16. G. S. Romanov, L. K. Stanchits and K. L. Stepanov, Tables of mean group absorption coefficients for aluminum plasma, BelNIINTI, Dept. No. 837Be-D84 (1984).
17. F. N. Borovick, S. I. Cas'cova, G. S. Romanov and K. L. Stepanov, Optical properties of bismuth plasma, *Zh. Prikl. Spektrosk.* **39**(6), 923–929 (1983).
18. Yu. S. Boyko, Yu. M. Grishin, A. S. Kamrukov and N. P. Kozlov, *Thermodynamic and Optical Properties of Plasma of Metals and Dielectrics.* Metallurgiya, Moscow (1988).
19. S. S. Katsnel'son and G. A. Koval'skaya, *Thermodynamic and Optical Properties of Argon Plasma.* Nauka, Novosibirsk (1985).
20. F. N. Borovick, S. I. Cas'cova, G. S. Romanov and K. L. Stepanov, The equation of state and the absorption coefficients of xenon plasma, VINITI, Dept No. 6022, No. 6023, Parts I, II (1982).
21. Yu. S. Boyko, Yu. M. Grishin, A. S. Kamrukov and N. P. Kozlov, *Thermodynamic and Optical Properties of Ionized Gases at Temperatures up to* 100 *eV.* Nauka, Moscow (1988).
22. V. I. Derjiev, A. G. Zhidkov and S. I. Yakovlenko, *Radiation of Ions in Nonequilibrium Dense Plasma.* Energoatomizdat, Moscow (1986).
23. V. E. Fortov and I. T. Yakubov, *Nonideal Plasma Physics.* Chernogolovka, Moscow (1982).
24. L. V. Gurvich, I. V. Veits and V. A. Medvedev, *Thermodynamic Properties of Individual Materials. Handbook,* Vols 1–4. Nauka, Moscow (1979).
25. A. A. Radtsig and B. M. Smirnov, *Handbook on Atomic and Molecular Physics.* Atomizdat, Moscow (1980).
26. K. P. Huber and G. Herzberg, *Molecular Spectra and Molecular Structure.* IV. *Constants of Diatomic Molecules.* Van Nostrand Reinhold, New York (1979).
27. C. Moore, *Atomic Energy Levels.* Vols 1, 2. NSRDS-NBS, Washington, DC (1949).
28. *Thermophysical Properties of Chemically Reacting Heterogeneous Mixture.* Collected papers of the Power Engineering Institute, Issue 7, Moscow (1973).
29. G. S. Romanov and L. K. Stanchits, About the calculation of thermodynamic gas parameters from the full system of the Saha equations, *Dokl. Akad. Nauk BSSR* **15**(3), 204–205 (1971).
30. V. A. Casiyanov and A. N. Starostin, On the theory of bremsstrahlung radiation of slow electrons on atoms, *Zh. Eks. Teor. Fiz.* **48**(1), 295–302 (1965).
31. O. B. Firsov and M. I. Chibisov, Bremsstrahlung radiation of slow electrons on neutral atoms, *Zh. Eks. Teor. Fiz.* **39,** No. 6(12), 1770–1776 (1960).
32. V. A. Kamenshchikov, Yu. A. Plastinin, V. M. Nikolaev

and L. A. Novitskii, *Radiation Properties of Gases at High Temperatures*. Mashinostroyeniye, Moscow (1971).
33. J. R. Stallcop and K. W. Billman, Analytical formulae for the inverse bremsstrahlung absorption coefficients, *Plasma Phys.* **16,** 1187–1189 (1974).
34. S. I. Cas'cova, G. S. Romanov, K. L. Stepanov and V. I. Tolkach, Thermophysic and optical properties of highly charged air plasma, Report at the 1st All-Union Symposium, *Radiation Plasmadynamics*, p. 73. Moscow (1989).
35. H. A. Bethe and E. E. Salpeter, *Quantum Mechanics of One- and Two-electron Atoms*. Springer, Berlin (1957).
36. A. Burgess and M. J. Seaton, A general formula for the calculation of atomic photoabsorption cross sections. *Mon. Not. R. Astron. Soc.* **120,** No. 2, 121–151 (1960).
37. F. N. Borovick, G. S. Romanov and K. L. Stepanov, Cross sections of continuous absorption of highly charged carbon plasma, VINITI, Dept No. 4912 (1981).
38. V. P. Stulov and V. N. Mirskii, Flow past the front surface of a body with intense evaporation under the action of radiation heating, Report No. 1416 of the Institute of Mechanics, Moscow State University, Moscow (1972).
39. S. T. Surzhikov, Computational models of radiative and gas-dynamic processes in a low-temperature plasma, Doctoral Dissertation, Institute for the Problems of Mechanics, Moscow (1990).
40. K. Watanabe, Processes of absorption of ultraviolet radiation in the upper atmosphere. In *Research of the Upper Atmosphere with Rockets and Satellites*, pp. 280–358. IL (1961).
41. B. E. Cole and R. N. Dexter, Empiric photoabsorption cross section for C, N, O, F and Cl obtained from molecular measurements between 50 and 340 A. *J. Quant. Spectrosc. Radiat. Transfer* **19,** 467–471 (1978).
42. A. H. Mnatsacanyan, Photodissociation and photoionization of diatomic molecules at high temperatures, *Teplofiz. Vysok. Temp.* **6,** No. 2, 236–241 (1968).
43. H. Griem, *Broadening of Spectral Lines in Plasma*. Nauka, Moscow (1978).
44. L. A. Kuznetsova, N. E. Kuz'menko, Yu. Ya. Kuzyakov and Yu. A. Plastinin, *Probabilities of Optical Transitions of Diatomic Molecules*. Nauka, Moscow (1980).
45. Yu. A. Plastinin and G. G. Baula, Absorption cross sections of electron bands systems of diatomic $N_2, O_2, N_2^+, NO, C_2, CN$ molecules at high temperatures. In *Physical Gasdynamics Studies*, pp. 41–61. Nauka, Moscow (1966).
46. G. Herzberg, *Molecular Spectra and Molecular Structure*. III. *Electronic Spectra and Electronic Structure of Polyatomic Molecules*. Toronto (1966).
47. H. Okabe, *Photochemistry of Small Molecules*. Wiley, New York (1978).
48. A. P. Zuev and A. Yu. Starikovskij, Absorption cross section of O_2, NO, N_2O, CO_2, H_2O, NO_2 molecules in the UV region of spectrum, *Zh. Prikl. Spektrosk.* **52**(3), 455–465 (1990).
49. N. I. Moskalenko, Yu. A. Il'in and N. K. Pokotilo, Effect of temperature on integral intensities of vibrational–rotational bands of absorption of steam and carbon dioxide, *Zh. Prikl. Spektrosk.* **34**(3), 475–480 (1981).
50. G. S. Romanov, Yu. A. Stankevich, L. K. Stanchits and K. L. Stepanov, Thermodynamic properties, spectral and mean absorption coefficients of gases in a wide range of parameters, Preprint No. 6 of the Heat and Mass Transfer Institute, Minsk (1993).
51. L. M. Biberman and G. E. Norman, Continuous absorption spectra of atomic gases and plasma, *Uspekhi Fiz. Nauk* **91,** No. 2, 193–246 (1967).